Int J Adv Manuf Technol (2008) 37:513–522
DOI 10.1007/s00170-007-0982-3

ORIGINAL ARTICLE

Modeling and optimization of Nd:YAG laser micro-weld process using Taguchi Method and a neural network

Hsuan-Liang Lin · Chang-Pin Chou

Received: 28 June 2006 / Accepted: 19 February 2007 / Published online: 10 March 2007

Abstract The use of a pulsed Nd:YAG laser in the 0.1 mm- thick aluminum alloy lap micro-weld process was optimized. The welding parameters that influence the quality of the pulsed Nd:YAG laser lap micro-weld were evaluated by measuring of the tensile-shear strength. In this work, the Taguchi method was adopted to perform the initial optimization of the pulsed Nd:YAG laser micro-weld process parameters. A neural network with a Levenberg-Marquardt back-propagation (LMBP) algorithm was then adopted to develop the relationships between the welding process parameters and the tensile-shear strength of each weldment. The optimal parameters of the pulsed Nd:YAG laser micro-weld process were determined by simulating parameters using a well-trained back-propagation neural network model. Experimental results illustrate the proposed approach.

Keywords Nd:YAG laser welding · Neural network · Taguchi method

1 Introduction

In the production of lithium-ion secondary batteries, the lap-welding of the safety vent and the cathode lead strongly influences the product quality and production efficiency. Laser spot welding is a micro-joining technique that is frequently used in the electronics industry. The pulsed Nd:YAG laser welding machine was employed herein. The pulsed Nd:YAG laser beam has a reputation for rapid, precise and easy welding. However, the technique is not effective in some applications [1]. Many parameters affect the quality of pulsed Nd:YAG laser welding, including pulse peak value, pulse width, pulse frequency, focus position, flow rate of shielding gas and others. The desired welding parameters are typically set from experience or a handbook. However, this approach does not ensure that the selected welding parameters result in optimal or near optimal welding quality for the particular welding system and environmental conditions.

The Taguchi method, a popular experimental design method in industry, can overcome the shortcomings of full factorial design when doing fractional factorial design. The approach optimizes parameter design, but with fewer experiments. Traditional experimental design is used to improve the mean level of a process such as the arithmetic mean of a sample. In modern quality engineering, experimental design work is performed to develop robust designs to improve the quality of the product. Taguchi's parameter design is intended to yield robust quality by reducing the effects of environmental conditions and variations due to the deterioration of certain components [2]. This high quality is achieved by the selection of various design alternatives or by varying the levels of the design parameters for component parts or system elements. It can optimize performance characteristics by the settings of design parameters and reduce the sensitivity of the system performance to sources of variation.

However, the Taguchi method has some limitations when adopted in practice. It can find optimal solutions

H.-L. Lin (✉)
Department of Vehicle Engineering, Army Academy, R.O.C.,
113, Sec.4, Jungshan E. Rd., Jungli,
Taoyuan, Taiwan 320,
Republic of China
e-mail: alaniin@ms47.hinet.net

C.-P. Chou
Department of Mechanical Engineering,
National Chiao Tung University,
Hsinchu 300, Taiwan

Table 1 Chemical concentration of each element in aluminum alloy, AA3003

Element	Si	Cu	Mn	Zn	Remain	Al
Wt-%	0.7	0.05~0.2	1.0~1.5	0.1	0.15	Balance

only within the specified level of control factors. After a parameter setting has been determined, the range of optimal solutions is set. The Taguchi method cannot find the real optimal values when the specified parameters are continuous, because it consider only discrete control factors.

A neural network is a non-linear function, and can accurately represent a complex relationship between inputs and outputs [3, 4]. A trained neural model has also been used to predict accurately the response (output) for specified parameter settings (input). Additionally, Khaw et al. [5] demonstrated that advantages can be gained using the Taguchi concept for neural network design. First, it is the only known method for neural network design that considers robustness as an important design criterion, increasing the quality of the neural network. Second, the Taguchi method uses orthogonal arrays (OAs) to design a neural network systematically, markedly reducing the design and development time for neural networks. This work combines the Taguchi method and a neural network to determine the optimal conditions for improving the quality of the Nd:YAG laser micro-weld process.

2 Initial optimization using Taguchi method

The safety vent and cathode lead used in the lithium-ion secondary batteries were made of AA3003 aluminum alloy (Please refer to Table 1 for its chemical composition). The safety vent had dimensions Ψ18×1.0 mm; the cathode lead had dimensions 3×70×0.1 mm. The pulsed Nd:YAG laser spot welding machine (Toshiba Lay-822H type) was employed in the experiment. The wavelength of the laser was 1.06 μm and via fiber conduction, the laser beam was used to join the product, in Fig. 1.

Fig. 2 Schematic of measurement for tensile-shear strength

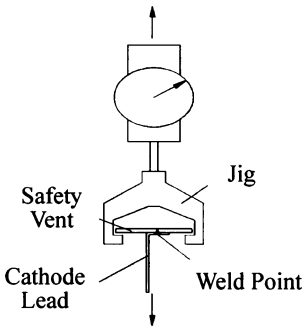

2.1 Quality characteristics of Nd:YAG laser micro-weld

The tensile-shear test is the most objective method for evaluating the spot weld characteristic of welding products. This work took the tensile-shear strength of specimens as the quality characteristic of the process. A tensile force testing instrument (IMADA MV-200BA type) was employed to measure the tensile-shear strength of the laser spot welding specimens. The speed was set to 6 in min^{-1} during testing. Figure 2 presents the measurement setup method. Weldment whose tensile-shear strength were lower than 0.5 kg were regarded as defective products, as suggested by engineers at a company that manufactures lithium-ion secondary batteries in Taiwan. This work aims to increase the mean tensile-shear strength of the weldment to 1.0 kg and to reduce the defective rate to under 5% to prevent leakage from the "safety vent" and to improve production efficiency.

2.2 Parameters of the Nd:YAG laser welding

Many approaches are effective in determining the factors that can be considered include in the initial experiments. They include brainstorming, flowcharting, and cause-effect diagrams [6]. Figure 3 presents the cause-effect diagram for this process. The Taguchi method separates factors into two main groups- control factors and noise factors. Control factors can be controlled by a manufacturer during processing, while noise factors are expensive and difficult to control [7]. As revealed by the literature [8] and

Fig. 1 Illustration of specimen and Nd:YAG laser welding facility (**a**) Specimen (**b**) Lens and jigs

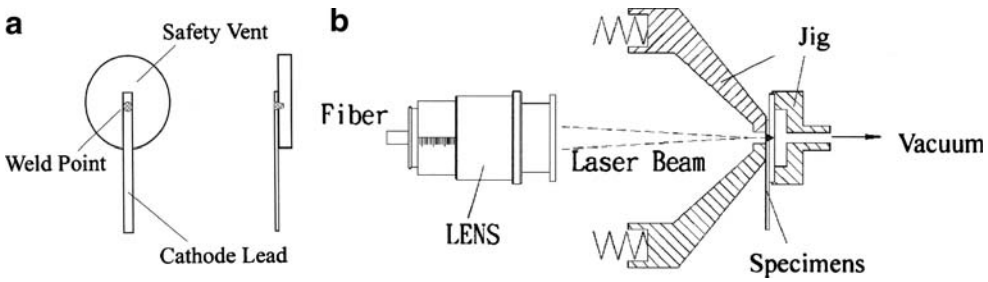

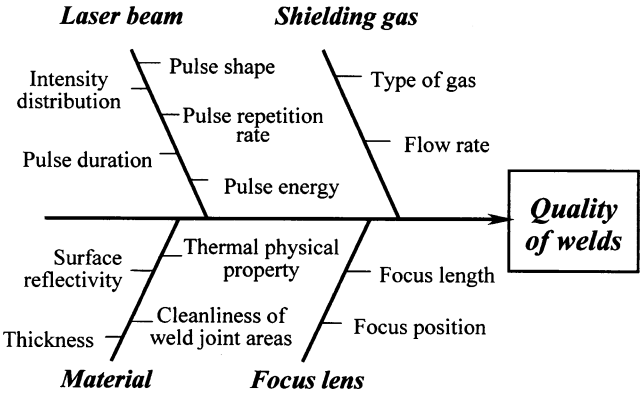

Fig. 3 Cause-effect diagram of Nd:YAG laser welding process

experience of production of lithium-ion secondary batteries, the most important welding parameters that determine the pulsed Nd:YAG laser spot welding quality of a weldment are pulse peak value, pulse width, pulse frequency and focus position. These parameters may be adjusted within the ranges, pulse peak value 0~500 V, pulse width 0.2~20.0 msec, pulse frequency 0.5~20 pps and focus position −1.0~+1.0 mm, respectively. Table 2 presents the various levels of the welding process parameters. The fundamental principle in robust design is to improve quality by minimizing the variation. Identifying important noise factors is critical to every robust design project [7]. Engineering experience and judgment are required to identify noise factors. Controlling the surface cleanliness of a weldment in automated production is difficult. Therefore, the cleanliness of the weld joint areas was used as the noise factor herein. Surface impurities were removed and the surface was cleaned using acetone at level one (N1). The specimens at level two (N2), which had not been cleaned, may have been tarnished with dirt and/or grease.

2.3 Orthogonal array experiment

One three-level and three five-level control factors, as well as one noise factor, were considered in this work. The interaction effect between the welding parameters is not considered. Therefore, the four control factors yield 14 degrees of freedom. The number of degrees of freedom for the OA should be at least the number of process parameters. The L25 (5^6) OA was employed in this work. The 'dummy level technique' was then adopted to change the L25 (5^6) OA into the L25 ($3^1 \times 5^3$) OA. Control factor A was assigned to column 1 of L25 OA using dummy levels $A_2=A_1'$, $A_3=A_2'$, $A_4=A_3'$ and $A_5=A_3'$. Other control factors (B~D) were assigned to column 2~4. Notably, orthogonality was preserved even when the dummy level technique was applied to one or more factors. Additionally, the noise factor was assigned to the outer array to determine the level of a control factor that does not cause much variation in the results, even though a noise factor is definitely present. Table 3 presents an experimental layout with an inner array for control factors and an outer array for a two-level noise factor (N1 and N2). The number of separate test conditions is 25×2=50; four repetitions for each trial (y_1, y_2, y_3 and y_4) were planned in this experimental arrangement; y_1 and y_2 are N1 specimens (cleaned with acetone), y_3 and y_4 are N2 specimens (without cleaning). In the Taguchi method, repetitions are

Table 2 Control factors and their levels

Factor	Process parameter	Level 1	Level 2	Level 3	Level 4	Level 5
A	Focus position, mm	−0.5	0	0.5	–	–
B	Pulse peak value, V	300	315	330	345	360
C	Pulse width, msec	4	5	6	7	8
D	Pulse frequency, pps	1	1.5	2	2.5	3

Table 3 Experimental layout using L25 orthogonal array

Trial no.	Control factor				Noise factor			
	A	B	C	D	N1 specimens		N2 specimens	
					y_1	y_2	y_3	y_4
1	1	1	1	1	Measure data			
2	1	2	2	2				
3	1	3	3	3				
4	1	4	4	4				
5	1	5	5	5				
6	1	1	2	3				
7	1	2	3	4				
8	1	3	4	5				
9	1	4	5	1				
10	1	5	1	2				
11	2	1	3	5				
12	2	2	4	1				
13	2	3	5	2				
14	2	4	1	3				
15	2	5	2	4				
16	3	1	4	2				
17	3	2	5	3				
18	3	3	1	4				
19	3	4	2	5				
20	3	5	3	1				
21	3	1	5	4				
22	3	2	1	5				
23	3	3	2	1				
24	3	4	3	2				
25	3	5	4	3				

Table 4 Experiment data

Trial no.	Tensile-shear strength, kg					
	y_1	y_2	y_3	y_4	Average	SNR, dB
1	0.05	0.10	0.01	0.01	0.04	−37.10
2	0.20	0.25	0.10	0.15	0.18	−16.66
3	0.70	0.64	0.50	0.40	0.56	−5.66
4	0.75	0.80	0.65	0.70	0.73	−2.87
5	0.85	1.00	0.80	0.75	0.85	−1.56
6	0.20	0.20	0.15	0.10	0.16	−16.87
7	0.35	0.55	0.30	0.45	0.41	−8.38
8	0.70	0.80	0.50	0.65	0.66	−3.97
9	0.40	0.25	0.35	0.20	0.30	−11.42
10	0.35	0.40	0.45	0.30	0.38	−8.82
11	0.25	0.20	0.20	0.15	0.20	−14.41
12	0.20	0.35	0.20	0.30	0.26	−12.39
13	0.15	0.20	0.15	0.10	0.15	−17.28
14	0.65	0.50	0.35	0.50	0.50	−6.66
15	0.50	0.65	0.40	0.60	0.54	−5.85
16	0.25	0.05	0.15	0.10	0.14	−21.46
17	0.30	0.35	0.40	0.20	0.31	−11.01
18	1.00	0.90	0.60	0.40	0.73	−4.50
19	0.60	0.70	0.50	0.65	0.61	−4.47
20	0.85	0.90	0.70	0.90	0.84	−1.68
21	0.35	0.30	0.10	0.20	0.24	−15.57
22	0.45	0.40	0.30	0.50	0.41	−8.18
23	0.55	0.50	0.35	0.50	0.48	−6.87
24	0.80	0.70	0.60	0.75	0.71	−3.10
25	0.80	0.95	0.70	0.85	0.83	−1.83

Total average of SNR for all trial is −9.942 (dB)

performed to assess the effect of noise on a quality characteristic(s) of interest.

2.4 Evaluation of initial optimal conditions

Taguchi proposed a method of transform repeated data to a single value of measures. The transformation is the signal-to-noise ratio (SNR) [6]. Several SNRs are available, depending on the type of characteristic being present. They include lower-is-better (LB), nominal-is-best (NB) and higher-is-better (HB). The tensile-shear strength of the specimens, as discussed earlier, is an HB quality characteristic. The SNRs, which condense multiple data points in a trial, depend on the characteristic that is being evaluated. The equation for the SNR ratio of HB characteristic is

$$SNR = -10 \log \left(\frac{1}{n} \sum_{i=1}^{n} \frac{1}{y_i^2} \right) \quad (1)$$

where n is the number of tests in a trial (which equals number of repetitions regardless of noise levels) and y_i is the tensile-shear strength of the specimens. The value of n is four in this work. Table 4 corresponds to the SNR of each trial. The effect of each welding process parameter on the SNR at various levels can be separated out because the experimental design is orthogonal. Table 5 describes the SNR for each level of each factor in the welding process.

Table 5 SNR response table for the tensile-shear strength

Factor	Process parameter	Level 1	Level 2	Level 3	Level 4	Level 5
A	Focus position	−11.329	−11.318	−7.867	–	–
B	Pulse peak value	−21.082	−11.323	−7.656	−5.701	−3.948
C	Pulse width	−13.049	−10.144	−6.646	−8.503	−11.368
D	Pulse frequency	−13.891	−13.464	−8.406	−7.433	−6.516

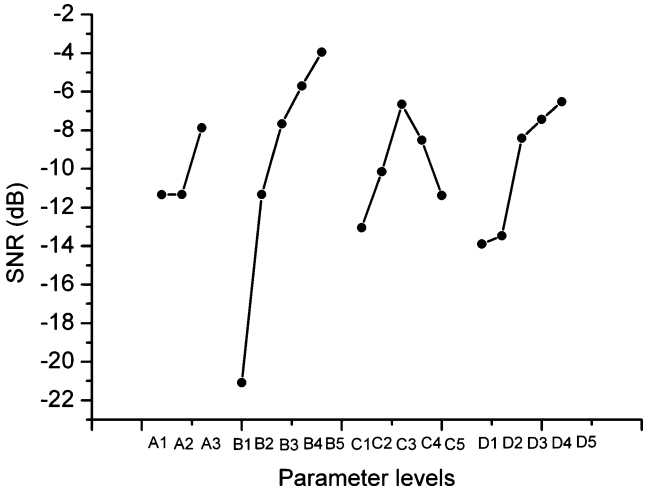

Fig. 4 SNR graph for the tensile-shear strength

Figure 4 plots the SNR graph obtained from Table 5. Basically, a larger SNR corresponds to a better quality characteristic (tensile-shear strength) of the specimens. The initial optimal combinations of the pulsed Nd:YAG laser micro-weld process parameter levels, $A_3B_5C_3D_5$, are obtained from Fig. 4.

2.5 Analysis of variance

The purpose of the analysis of variance (ANOVA) is to investigate the welding process parameters, which significantly affect quality [6]. The percentage contribution to the total sum of squared deviations can be used to evaluate the importance of a change in a welding process parameter on these quality characteristics. The F-test can also be adopted to determine which welding process parameters significantly affect the quality characteristics. Usually, when the F-Test value exceeds four, a change in the process parameter significantly affects the quality characteristics [9]. The pulse peak value, the pulse frequency and the focus position are welding parameters that significantly affect the quality characteristic (tensile-shear strength of each specimen): the pulse peak value is the most important, as shown in Table 6.

2.6 Confirmation tests for initial optimization

The final step is to compare the estimated value with the confirmative experimental value, using the optimal levels of the control factors to confirm experimental reproducibility. The estimated SNR η_{opt} using the optimal level of the control factors, is calculated as

$$\eta_{opt} = \widehat{\eta} + \sum_{j=1}^{q} (\eta_j - \widehat{\eta}) \tag{2}$$

where $\widehat{\eta}$ is the total average SNR of all the experimental values, η_j is the mean SNR at the optimal level, and q is the number of the control factors that significantly influence the quality characteristic. Tables 4 and 5 reveal that factor C has the least effect on the quality characteristic. In order to prevent an over-estimate [2], factor C is not considered and the estimated SNR η_{opt} is computed as

$$\begin{aligned}\eta_{opt} &= -9.942 + (-7.867 + 9.942) + (-3.948 + 9.942) \\ &\quad + (-6.516 + 9.942) \\ &= 1.553(dB)\end{aligned}$$

A confidence interval (CI) is a range between the maximum and minimum values. The true average has some stated percentage of confidence [6]. The confidence limits on the above estimation can be calculated using the following equation

$$CI = \sqrt{F_{\alpha,\nu_1,\nu_2} V_{ep} \left(\frac{1}{n_{eff}} + \frac{1}{r}\right)} \tag{3}$$

where F_{α,ν_1,ν_2} is the F-ratio required for α=0.05 (with a confidence of 95%); ν_1 is the number of degrees of freedom of the mean (which always equals one); ν_2 is the number of degrees of freedom of the error; V_{ep} is the error variance; r is the sample size in the confirmation experiment, and n_{eff} is the effective sample size.

$$n_{eff} = \frac{N}{1 + DOF_{opt}} \tag{4}$$

Table 6 Results of ANOVA for the tensile-shear strength

Factor	Process parameter	Degree of freedom	Sum of square	Mean square	F-test	Pure sum of square	Percent contribution
A	Focus position	2	196.049	98.025	19.75	186.12	12.11%
B	Pulse peak value	4	925.757	231.439	46.63	905.90	58.95%
C	Pulse width	4	123.328	30.832	6.21	103.47	6.73%
D	Pulse frequency	4	241.943	60.486	12.19	222.09	14.45%
Error		10	49.636	4.964		119.13	7.75%
Total		24	1536.71			1536.71	100%

Table 7 Results of the confirmation experiment

Trial no.	Tensile-shear strength						Confidence interval, 95%
	N1 specimens		N2 specimens		SNR, dB	Average, kg	
26	0.96	1.05	0.83	0.92	−0.63	0.933	1.553±4.364 (dB)
27	1.05	1.00	0.90	0.83	−0.60	N1=1.008	
28	1.02	0.97	0.82	0.85	−0.88	N2=0.858	

where N is the total number of trials, and DOF_{opt} is the total degrees of freedom that are associated with the items used to estimate η_{opt}.

Given a CI of 95% for the tensile-shear strength, $F_{0.05,1,10}$=4.96, and V_{ep}=4.964, the sample size in the confirmation experiment r is 3, N=25, DOF_{opt}=10, and the effective sample size n_{eff} is 2.273. Therefore, the CI is computed to be CI=4.364 (dB). The experimental results (Table 7) confirm that the initial optimizations of the Nd: YAG laser micro-weld process parameters were achieved.

3 Neural network with Levenberg-Marquardt back propagation algorithm

Neural networks are used to model complex manufacturing processes, typically for process and quality control [10, 11]. Many well-known supervised learning networks are back propagation (BP) neural networks. Funahashi [12] demonstrated that the BP neural network may approximately realize any continuous mapping. Back propagation learning employs a gradient descent algorithm to minimize the mean square error between the target data and the predictions of a neural network. However, one of the major problems with the basic BP algorithm (gradient descent algorithm) is the extended training time required. Approaches for accelerating convergence fall into two main categories - heuristic and standard numerical optimization. The latter includes the Levenberg-Marquardt back-propagation (LMBP) algorithm [13].

The LMBP algorithm is similar to the quasi-Newton method, in which a simplified form of the Hessian matrix (second derivatives) is used. From Taylor series, of a generic function $F(x)$, the following can be written [13–15].

$$F(x_{k+1}) = F(x_k + \Delta x_k) \cong F(x_k) + G(x,k)\Delta x_k + \frac{1}{2}\Delta x_k H(x,k)\Delta x_k \quad (5)$$

where $G(x,k)$ is the gradient of $F(x)$, Δx_k is $x_{k+1} - x_k$ and $H(x,k)$ is the Hessian matrix of $F(x)$.Differentiating Eq. (5) with respect to Δx_k yields Eq. (6).

$$G(x,k) + H(x,k)\Delta x_k = 0 \quad (6)$$

This equation can be re-written in the following form.

$$\Delta x_k = -H(x,k)^{-1} G(x,k) \quad (7)$$

Table 8 Options for different networks

Architecture (input-hidden unit-output)	Mean square error for training	Simulating error, % (compare with average value in Table 7)	
		N1 value	N2 value
5-2-1	0.0077	−20.6	−16.6
5-3-1*	0.0046	−26.2	−19.1
5-4-1	0.0121	−14.1	−8.2
5-5-1	0.0052	−21.3	−21.4
5-6-1	0.0078	−21.9	−10.5
5-7-1	0.0304	−25.0	−37.9
5-8-1	0.0119	−31.6	−29.7
5-9-1	0.0064	−24.5	−24.3
5-10-1	0.0083	−16.0	−22.6
5-15-1*	0.0027	5.1	−13.1
5-20-1	0.0099	−33.2	−19.0
5-25-1*	0.0027	−33.7	−62.2
5-30-1	0.0243	−50.9	83.2
5-35-1*	0.0034	−22.9	−33.4
5-40-1*	0.0020	−20.8	−50.6

*The structures are the five best convergence criteria

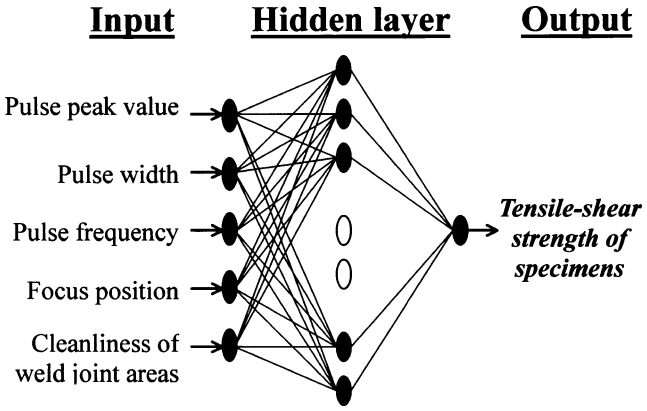

Fig. 5 Configuration of the BP network for modeling of the Nd:YAG laser welding process

The updating rule for the Newton algorithm is then obtained.

$$x_{k+1} = x_k - H(x,k)^{-1}G(x,k) \tag{8}$$

Consider a generic quadratic function as the objective function, represented by Eq. (9) for a multi-input multi-output system. (The iteration index is omitted and i is the index of the outputs.)

$$F(x) = \sum_{i=1}^{N} e_i^2(x) \tag{9}$$

Then,

$$G(x) = J^T(x)e(x) \tag{10}$$

$$H(x) = J^T(x)J(x) + S(x) \tag{11}$$

where $J(x)$ is the Jacobian matrix and $S(x)$ is

$$S(x) = \sum_{i=1}^{N} e_i(x)\nabla^2 e_i(x) \tag{12}$$

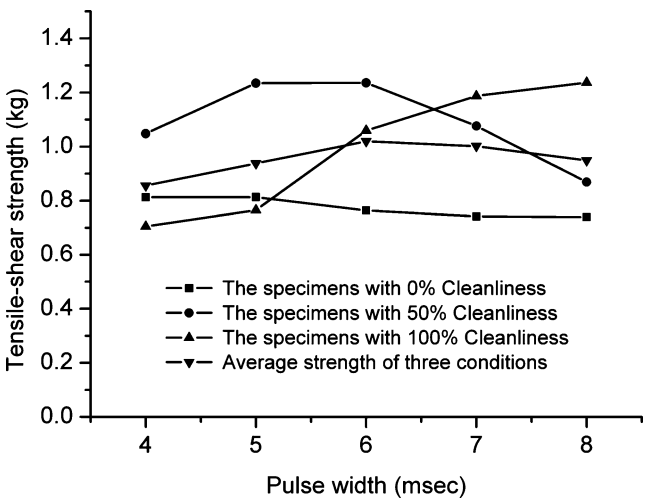

Fig. 6 Results of simulating different pulse width and cleanliness

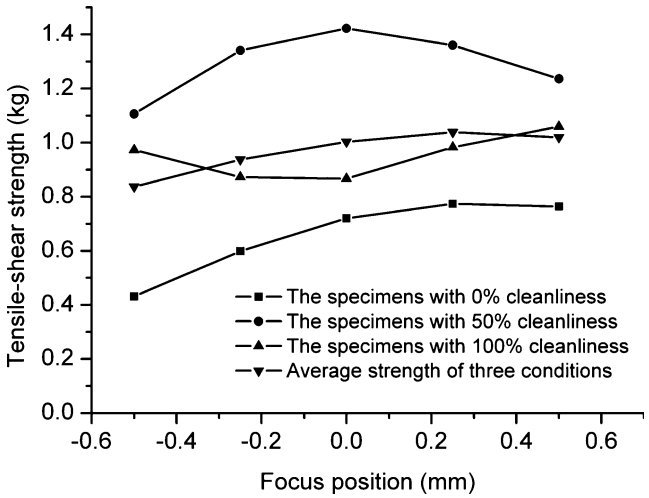

Fig. 7 Results of simulating different focus position and cleanliness

$S(x)$ is assumed to be smaller than compared to the product of the Jacobian, and the Hessian matrix can be approximated by the following.

$$H(x) \approx J^T(x)J(x) \tag{13}$$

This approach can update Eq. (8) and yields the Gauss-Newton algorithm

$$\Delta x_k = \left[J^T(x)J(x)\right]^{-1}J^T(x)e(x) \tag{14}$$

One limitation that can of this algorithm is that the simplified Hessian matrix may not be invertible. A modified Hessian matrix can be used to solve this problem.

$$Hm(x) = H(x) + \mu I \tag{15}$$

where I is the identity matrix and μ is a value that makes $Hm(x)$ positive definite, and therefore invertible. This last change in the Hessian matrix corresponds to the Levenberg-Marquardt algorithm.

$$\Delta x_k = \left[J^T(x)J(x) + \mu I\right]^{-1}J^T(x)e(x) \tag{16}$$

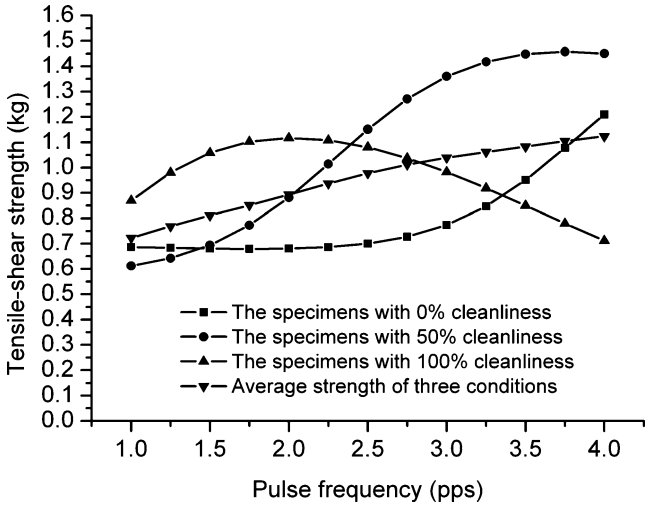

Fig. 8 Results of simulating different pulse frequency and cleanliness

When the scalar μ is zero, it is just Gauss-Newton, using the approximate Hessian matrix. When μ is large, this descends in small steps. The algorithm begins with μ set to some small value (such as μ=0.01). If a step does not yield a smaller value for e, then it is repeated with μ multiplied by some factor θ>1 (such as θ=10). Eventually, e decreases, since a small step is being taken in the direction of steepest descent. If a step yields a smaller e, then μ is divided by θ in the next step, ensuring that the algorithm approaches Gauss-Newton, accelerating convergence [13]. The LMBP algorithm is the fastest algorithm that has been tested for training multiplayer networks of moderate size, even though it requires a matrix inversion at each iteration. It requires two parameters, but the algorithm does not appear to be sensitive to this selection. Additionally, Kumar et al. demonstrated [16] that the LMBP algorithm and Gauss-Newton were performed best for least square problems. In particular, the LMBP algorithm performs better than the Gauss-Newton method when the initial estimate is poor. In summary, the LMBP algorithm provides a favorable compromise between the speed of Newton's method and the guaranteed convergence of steepest descent.

4 Application of back propagation neural network

4.1 Training of back propagation network

A neural network, which can capture and represent the relationship between the process variables and process outputs, was developed in this stage. Multilayer perceptions are feedforward neural networks are commonly used to solve difficult predictive modeling problems [17]. They typically consist of an input layer, one or more hidden layers, and one output layer. The neurons in the hidden layers are computational units that perform non-linear mapping between inputs and outputs. A feedforward neural network was adopted in this work. It takes a set of five input values (control factors A, B, C, D and noise factor) and predicts the value of one output (tensile-shear strength of each specimen). The transfer functions of all hidden neurons are tangent sigmoid functions. The transfer functions of the output neurons are linear functions [18].

Determining the number of hidden neurons is critical to the design of neural networks. An over-abundance of hidden neurons provides too much flexibility, which typically causes overfitting. However, too few hidden neurons restrict the learning capacity of a network and degrade its approximation performance [17]. A total of 100 input-output data patterns were separated into a training set, a testing set and a validating set. Functionally, 60% (60 patterns) were randomly selected to train the neural network; 20% (20 patterns) were selected randomly for testing and 20% (20 patterns) were selected randomly for validating. An efficient algorithm, the Levenberg-Marquardt algorithm, was adopted to improve classical BP learning in the training process [13, 17]. The neural network software MATLAB Neural Network ToolBox was used to develop the required network.

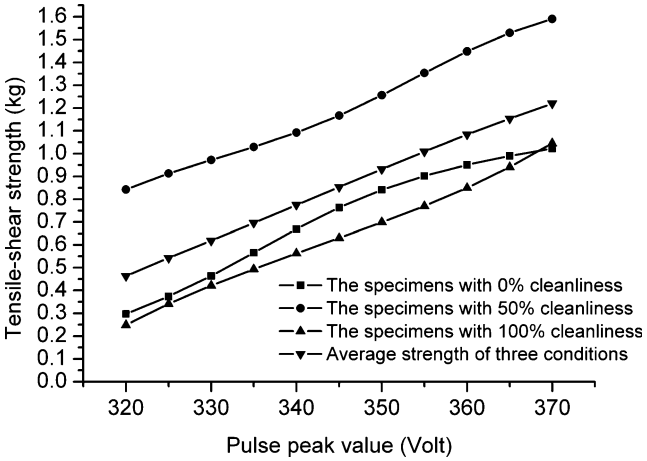

Fig. 9 Results of simulating different pulse peak value and cleanliness

Table 8 presents 15 options for the neural network architecture. Comparing all of the data for the mean square error (MSE) reveals that the structures 5-3-1, 5-15-1, 5-25-1, 5-35-1 and 5-40=1 are the five best for convergence. The structure 5-15-1 yielded the smallest error and was therefore adopted to obtain a better performance. Figure 5 presents the topology of the network 5-15-1 with a μ value of 0.001 and a θ value of 10.

4.2 Optimization with a well-trained network

The control factor C (pulse width) is an insignificant welding parameter that affect the quality characteristic (tensile-shear strength of each specimen), as shown in Table 6. First, the trained network 5-15-1 was employed as the simulating function of the control factor C. Figure 6 compares the results simulated using the pulse width, other conditions $A_{+0.5\ mm}B_{360\ V}D_{3\ pps}$, indicating that the tensile-

Table 9 Results of the proposed approach

Trial no.	Tensile-shear strength				
	N1 specimens		N2 specimens		Average, kg
29	1.05	1.14	0.94	0.90	1.013
30	1.00	1.07	1.00	0.96	N1=1.063
31	1.10	1.02	0.92	1.05	N2=0.962

Table 10 A comparison of each condition

	Focus position, mm	Pulse peak value, V	Pulse width, msec	Pulse frequency, pps	Defective rate, %	Average, kg
Initial condition	0	330	6	2	8.67	0.886
Taguchi method	+0.5	360	6	3	5.37	0.979
Proposed approach	+0.25	355	6	3.4	2.00	1.023

Sample size of comparison: 150

shear strength of specimens is optimal for setting the pulse width to 6 msec.

Second, Fig. 7 compares the results simulated using the factor A, other conditions $B_{360\ v}C_{6\ ms}D_{3\ pps}$, indicating that the tensile-shear strength of the specimens is best when the focus position is adjusted from +0.5 to +0.25 mm.

Third, Fig. 8 compares the results simulated using factor D, other conditions $A_{+0.25\ mm}B_{360\ v}C_{6\ ms}$, indicating that the pulse frequency and tensile-shear strength are in direct proportion. As the pulse frequency rises over 2.0 pps, the tensile-shear strength declines for N1 specimens (with 100% cleanliness). However, it increase for N2 specimens (with 0% cleanliness). In this work, the pulse frequency was set to 3.4 pps.

Finally, Fig. 9 compares the results simulated using the factor B and other conditions $A_{+0.25\ mm}C_{6\ mse}D_{3.4\ pps}$, indicating that the pulse peak value and tensile-shear strength are in direct proportion. As the pulse peak value rises over 355 V, the tensile-shear strength of the specimens approaches 1.0 kg. Additionally, Fig. 9 reveals that the specimens with 50% cleanliness are better than both the N1 (with 100% cleanliness) and the N2 (with 0% cleanliness) specimens.

4.3 Experimental results of Proposed Approach

Combining the Taguchi method and neural networks yielded the welding condition that optimized the tensile-shear strength of an Nd:YAG laser weldment: focus position=+0.25 mm, pulse peak=355 V, pulse frequency= 3.4 pps and pulse width=6 msec. Table 9 presents the experimental results obtained using these optimal welding parameters. Comparing Table 7 with 9 reveals that the improvement in the average tensile-shear strength of N2 specimens (without cleaning) when the initial optimal parameters are change to the real optimal parameters is 0.104 kg. The defective rate of the optimal welding parameters with the proposed approach is lower than that obtained using the Taguchi method only, as shown in Table 10. In summary, the proposed approach efficiently improves the quality of the Nd:YAG laser micro-weld process.

5 Conclusions

The results in this work support the following conclusions:

1. The improvement of the defective rate from the initial conditions to the initial optimal parameters (obtained using the Taguchi method) is 3.34%; that from the initial conditions to the real optimal parameters (obtained using the proposed approach) is 6.67 %.
2. The results obtained by simulation using a well-trained neural network model reveal that the specimens (AA3003 aluminum alloy) with 50% cleanliness contributed most tensile-shear strength to the Nd:YAG laser micro-weld process. The cleaning treatment of the safety vent and the cathode lead of the lithium-ion secondary batteries must be corrected to improve the welding quality.

Acknowledgment The authors acknowledge Mr. Sheng-Lee Tsai, the Section Manager of Production Technology Dept. of Pacific Energytech Co., Ltd. in Taiwan, for sharing his expertise and permitting the use of the Nd:YAG laser micro-weld technical data in this study.

References

1. Pan LK, Wang CC, Hsiao YC, Ho KC (2004). Optimization of Nd:YAG laser welding onto magnesium alloy via Taguchi analysis. Opt Laser Technol 37:33–42
2. Taguchi G (1993) Taguchi methods: Design of experiments. American Supplier Institute, Inc., MI
3. Su CT, Chiu CC, Chang HH (2000) Parameter design optimization via neural network and genetic algorithm. Int J Ind Eng 7(3):224–231
4. Kim IS, Jeong YJ, Lee CW (2003) Prediction of welding parameters for pipeline welding using an intelligent system. Int J Adv Manuf Technol 22:713–719
5. Khaw JFC, Lim BS, Lim LEN (1995) Optimal design of neural networks using Taguchi method. Neurocomputing 7:225–245
6. Ross PJ (1988) Taguchi Techniques for Quality Engineering. McGraw-Hill, New York
7. Phadke MS (1989) Quality engineering using Robust design. Prentice-Hall, Upper Saddle River, NJ
8. Yu T (2002) Study on the pulse Nd:YAG laser welding for packaging process parameters. National Tsing Hua University (Taiwan), Thesis, pp49–52.

9. Roy RK (1990), A primer on the Taguchi method. Reinhold, New York
10. Su CT, Chiang TL (2003) Optimizing the IC wire bonding process using a neural networks/genetic algorithms approach. J Intell Manuf 14:229–238
11. Coit DW, Jacson BT, Smith AE (1998) Static neural network process model: considerations and cases studies. Int J Prod Res 36 (11):2953–2967
12. Funahashi K (1989) On the approximate realization of continuous mapping by neural network. Neural Netw 2:183–192
13. Hagan MT, Demuth H, Beale M (1996) Neural network design. PWS , Boston, MA
14. Hagan MT, Menhaj MB (1994) Training feedforward networks with the Marquardt algorithm. IEEE Trans Neural Netw 5(6):989–993
15. Dias FA, Antunes A, Vieira J, Mota A (2006) A sliding window solution for the on-line implementation of the Levenberg-Marquardt algorithm. Eng Appl Artif Intell 19:1–7
16. Kumar K, Alsaleh MA (1996) A comparative study for the estimation of parameters in nonlinear models. Appl Math Comput 77:179–183
17. Haykin S (1994) Neural networks-a comprehensive foundation. Macmillan College Publishing, New York
18. Demuth H, Beale M (1998) Neural network toolbox-for use with MATLAB. The Math Works, Inc., Boston, MA